JOURNAL OF PROPULSION AND POWER
Vol. 24, No. 5, September–October 2008

Desensitization of the Flowfield from Rotor Tip-Gap Height by Casing-Air Injection

Thomas Behr*
ETH Zurich, 8092 Zurich, Switzerland
Anestis I. Kalfas†
Aristotle University of Thessaloniki, 541 24 Thessaloniki, Greece
and
Reza S. Abhari‡
ETH Zurich, 8092 Zurich, Switzerland

DOI: 10.2514/1.34891

This paper presents an investigation that aims to desensitize the flowfield of an unshrouded high-pressure gas-turbine stage from the radial clearance between the rotor tip and the casing. A novel method of cooling-air injection from the rotor casing into the rotor tip region is applied. The injection opposes the tip-leakage flow and affects the development of the rotor secondary flow. In a previous investigation, an increase of stage efficiency of 0.55 percentage points was achieved with an injection of 0.7% of the core mass flow. The present study investigates the effect of the injection on the flowfield for two different rotor tip clearances. Measurements conducted with a two-sensor fast-response pressure probe provide data describing the time-resolved behavior of flow angles and pressures as well as turbulence intensity. The experimental investigation is done on the tip-gap heights of 0.65 and 1.00% span and injection mass flow rates representing 0, 0.7, and 1% of the turbine core mass flow. The results show that an increasing injection rate reduces the difference of rotor exit flow angle and flow unsteadiness between the two different tip-gap heights. The stage efficiency increases with injection for both tip-gap cases, whereas identical values are obtained at the injection rate of 1% of the turbine mass flow.

Nomenclature

BR	=	blowing ratio ($\rho_c c_c/\rho_m c_m$)
Cp	=	pressure coefficient $(p - p_{s,3})/(p_{t,0} - p_{s,3})$
c	=	absolute flow velocity, m/s
c_p	=	specific heat capacity at constant pressure, J/kg K
DR	=	density ratio (ρ_c/ρ_m)
$\dot{H}$	=	enthalpy flux, W
h	=	enthalpy, J/kg
IR	=	impulse ratio (BR^2/DR)
M	=	torque, N m
$\dot{m}$	=	mass flow, kg/s
p	=	pressure, Pa
r	=	radius, m
T	=	temperature, K
Tu	=	turbulence intensity, %
TKE	=	turbulent kinetic energy, J/kg
u	=	rotor velocity, m/s
v	=	rotor-relative velocity, m/s
η	=	efficiency
κ	=	isentropic coefficient (c_p/c_v)
ρ	=	density, kg/m^3
σ	=	standard deviation
ψ	=	loading coefficient ($\Delta h/u^2$)
ϕ	=	flow coefficient (c_x/u)

Subscripts

c	=	coolant jet
I	=	rotor injection flow
is	=	isentropic
M	=	first-stage main inlet flow
m	=	local main flow
r	=	radial coordinate
rel	=	rotor-relative
s	=	static
sw	=	streamwise coordinate
T	=	first-stage total exit flow
t	=	total
w	=	wall
x	=	axial coordinate
θ	=	circumferential coordinate
0	=	turbine inlet
3	=	turbine exit

Superscripts

$\bar{}$	=	mass average
$'$	=	turbulent fluctuation

Introduction

AN AEROENGINE represents a complex system of components that has to operate under extreme structural and thermal conditions. Moreover, transient loads occur when the operating mode of the machine is changed. In such cases, the changing gas temperatures cause an expansion or contraction of adjoining metal parts. Tolerances and gaps between parts have to be designed in a way to be able to cope with these varying load conditions. One critical dimension in the turbine of an aeroengine is the radial gap between the rotor blade tip and the casing. Depending on the thermal expansion of the rotor and the casing parts, the tip gap will change in height. According to the influence of the tip-gap flow, the flowfield of the rotor and the downstream stator will adjust and deviate from the

Received 3 October 2007; revision received 17 March 2008; accepted for publication 18 March 2008.

*Turbomachinery Laboratory; thomas.behr@gmx.net.
†Department of Mechanical Engineering.
‡Turbomachinery Laboratory.

design intention. Because rotor losses due to tip leakage contribute to as much as one-third of the overall blade-row loss (Booth [1]), it is desirable to control them.

According to Wiseman and Guo [2], in a high-pressure turbine of an aircraft engine, a reduction of the rotor tip clearance of about 0.25 mm would reduce the specific fuel consumption (which is the mass of fuel needed to provide a given power for a given period) by about 1%. However, the reduction of the radial tip-gap height is limited, because the clearance between the blade tips and the surrounding casing tends to vary due to changes in thermal and mechanical loads on the rotating and stationary structures. In aeroengines, the tip sealing is even more complicated due to frequently changing operating points and inertial and aerodynamic loads during flight maneuvers. The tip clearance reaches a minimum value during the takeoff phase. The centrifugal force on the rotor and the unequal thermal expansion of the rotor and the casing are responsible for the tip-clearance reduction. In engines of large commercial planes, the change of tip clearance can be around 0.76 mm [3] during takeoff and reacceleration events.

On the effect of tip leakage in a multistage environment, Harvey [4] concluded that no benefit results from the tip-leakage flow once it has formed into a vortex. To limit the losses that this vortex generates in subsequent blade rows, the tip-leakage flow and thus the strength of the vortex have to be reduced. According to Denton [5], the loss related to the tip-leakage flow is proportional to a discharge coefficient, which depends on the velocity distribution around the blade tip, and thus on the loading of the blade tip. The leakage mass flow is further dependent on the through flow area and thus on the tip-gap height. These two main aspects, the reduction of rotor tip loading and the minimization of the radial tip gap, have been the subject of a number of investigations in past decades, to reduce the losses due to tip leakage.

One way of changing the discharge coefficient without significantly affecting the pressure distribution around the tip profile is to modify the blade tip geometry. Contouring can be done by including squealer rims or radii along the edges of the tip (Booth [6], Bindon and Morphis [7], Kaiser and Bindon [8], and Camci et al. [9]). Numerical analyses examining the influence of improved tip concepts have been presented by Mischo et al. [10], Tallman [11], Willer et al. [12], Schabowski and Hodson [13], and Chander et al. [14]. The possibility of reducing tip-leakage flows through a reduced loading of the tip region has been discussed by De Cecco et al. [15] and Yamamoto et al. [16]. Staubach et al. [17] achieved the offloading of the tip by applying 3-D design strategies to the profiles. Offenburg et al. [18] investigated the effect of different trenches within the casing around the rotor on the efficiency of the stage. All of the aforementioned approaches suffer from varying tip clearances during an operational cycle.

In the literature, a variety of strategies can be found to control the tip clearance around a rotor. Generally, the approaches can be categorized as either active clearance control or passive clearance control. Passive clearance control is defined as a system in which the tip clearance is set at one operating point, whereas active clearance control systems adjust the clearance at different operating points. An overview of the work in this field is given by Lattime and Steinetz [3]. Active thermal clearance controls represent the most common systems applied in gas-turbine engines. They use compressor discharge air to heat (expand) or cool (shrink) the supports of the rotor-casing segments [19,20]. Active mechanic [21] and active pneumatic [22] systems have also been investigated. However, their application in real engines is limited due to problems of actuators in the high-temperature environment and high-cycle fatigue. Passive thermal clearance controls rely on material properties and engine temperatures to match rotor and stator expansion and shrinking; however, these systems allow only an optimized tip clearance at one operating point: usually, at takeoff [23]. Passive pneumatic clearance controls are driven by engine-generated gas-pressure or hydrodynamic effects. This group also includes the injection of air from the rotor tip's pressure side, which opposes the flow direction of the tip leakage (Huber and Dietrich [24], Dey and Camci [25], and Rao and Camci [26]). The concept of injecting air from the rotor casing through circumferential slots onto the rotor blade tip was proposed by Auyer [27]. Minoda et al. [28] injected air in a similar way through arrays of inclined holes at three axial positions. The general problem that applies to all of these tip-clearance control systems is the correct adaptation of the rotor tip clearance to the respective engine operating condition. Furthermore, the system has to prove stable operation in a high-temperature environment.

Concluding from these considerations, it is desirable to have a system that makes the flowfield of the turbine insensitive to changes in the rotor tip clearance. Behr et al. [29] presented a novel method of cooling-air injection from the rotor casing into the tip region of the rotor blade. The injected air is used to oppose the leakage flow across the blade tip. It was experimentally shown that this method is able to reduce the tip leakage and the secondary flow in the rotor and to increase the stage efficiency. In the present paper, it is investigated how the casing-air injection influences the effect of tip-clearance changes.

Experimental Method

Turbine Test-Rig Facility

The experiments for the current investigation were conducted on the 1.5-stage unshrouded axial turbine test rig at the Turbomachinery Laboratory of ETH Zurich. A cross-sectional view of the turbine module is presented in Fig. 1. Global parameters of the turbine at the design operating point are shown in Table 1. The characteristics of each blade row are presented in Table 2.

The air loop of the facility is of a quasi-closed type and includes a radial compressor, a two-stage water-to-air heat exchanger, and a calibrated Venturi nozzle for mass flow measurements. Before the flow enters the turbine section, it passes through a 3-m-long straight duct, which contains flow straighteners to ensure an evenly distributed inlet flowfield. Downstream of the turbine the air loop is open to atmosphere. A dc generator converts the turbine power and controls the rotational speed of the turbine. A torque meter measures the torque that is transmitted by the rotor shaft to the generator. The

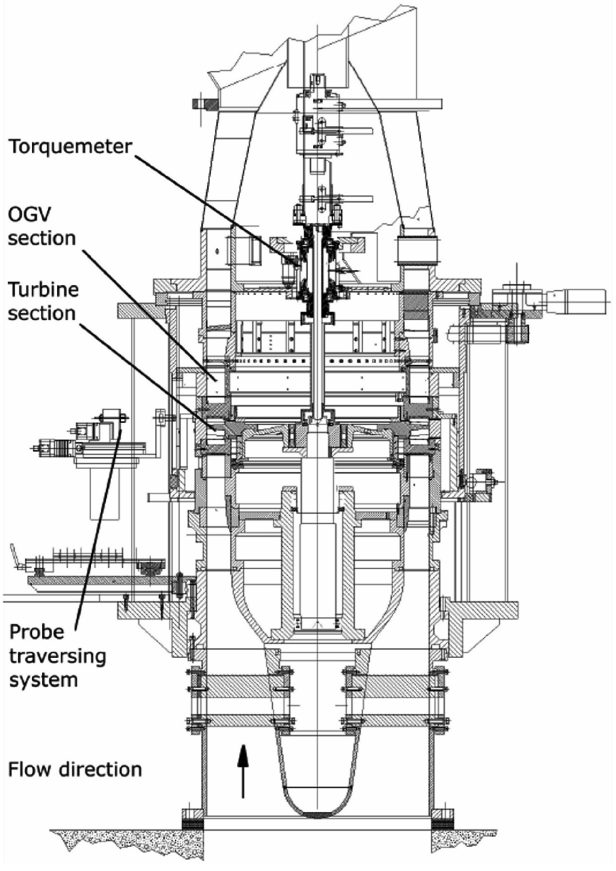

Fig. 1 Lisa 1.5-stage axial turbine facility.

Table 1 Main parameter of Lisa 1.5-stage axial turbine research facility at the design operating point (measured)

Turbine	
Rotor speed, rpm	2700
Pressure ratio (1.5-stage, total to static)	1.60
Turbine entry temperature, °C	55
Total inlet pressure, bar absolute norm	1.4
Mass flow, kg/s	11.7
Shaft power, kW	292
Hub/tip diameter, mm	660/800
First stage	
Pressure ratio (first stage, total to total)	1.35
Degree of reaction	0.39
Loading coefficient $\psi = \Delta h/u^2$	2.26
Flow coefficient $\phi = c_x/u$	0.56

Table 2 Characteristic geometry and performance parameters of the 1.5-stage turbine configuration

	Stator 1	Rotor	Stator 2
Number of blades	36	54	36
Inlet flow angle, deg (midspan)	0	54	−42
Exit flow angle, deg (midspan)	73	−67	64
Aspect ratio (span/chord)	0.87	1.17	0.82
Blade row relative exit Mach numbers (average)	0.54	0.50	0.48
Reynolds number based on true chord and blade row relative exit velocity	7.1×10^5	3.8×10^5	5.1×10^5

turbine entry temperature is controlled to an accuracy of 0.3%, and the rpm is kept constant within ± 0.5 min^{-1} by the dc generator. The pressure drop across the turbine is stable within 0.3% for a typical measurement day. More detailed information on the test rig can be found in [30].

Measurement Techniques

The flowfield data presented in the paper are derived from time-resolved probe measurements in a plane that is located 15% rotor axial chord downstream of the rotor trailing edge. The unsteady-pressure-measurement technology of the fast-response aerodynamic probes (FRAP) was developed at the Turbomachinery Laboratory of ETH Zurich (Kupferschmied et al. [31] and Pfau et al. [32]). The mainstream flowfield was measured using a novel 1.8-mm-tip-diam two-sensor FRAP probe in virtual-four-sensor mode to provide two-dimensional time-resolved flowfield information. Each measurement plane is resolved by a grid of 27 points in the radial direction clustered close to the endwalls and 20 equally spaced points in the circumferential direction, covering one stator pitch. The minimum distance between two measurement points is set by the probe tip diameter. The time-resolved pressures signals are acquired at each measurement point at a sampling rate of 200 kHz over a period of 2 s. The data sets are processed to derive basic flow quantities (i.e., total and static pressure, flow yaw and pitch angles, velocity components, and Mach number) by applying a phase-lock average over 85 rotor revolutions. For the data evaluation, three consecutive rotor passages are selected. Each rotor pitch is resolved in time by 82 samples. The frequency response of the probe allows flow features to be captured at frequencies up to 35 kHz. With this two-sensor probe technology, it is also possible to determine flow turbulence information (Porreca et al. [33]). The FRAP probe technology provides also temperature data at a frequency of up to 10 Hz.

Uncertainty Analysis

A detailed uncertainty analysis of all measurement techniques used for the investigation is presented by Behr [34]. The uncertainty analysis was done according to [35]. Unlike previously used methods, [34] describes a standardized method, which first converts all uncertainty information in probability distributions. Based on this, it is consistent to use only the Gaussian error-propagation formula to derive the overall uncertainty. In the case of correlated parameters, cross-correlation coefficients are used to evaluate their combined uncertainty contribution. Consequently, the final statement of uncertainty of the measurement result contains the limits and the distribution of the expected values. The range of uncertainty of the flow parameters measured with the FRAP technique for a confidence level of 1σ based on a normal distribution is presented in Table 3.

Table 3 Typical range of standard uncertainty (σ) according to [35] of flow parameters measured with FRAP

Parameters	Rotor exit ($Ma = 0.25$)	Stator exit ($Ma = 0.5$)
Flow yaw and pitch angle	±0.5 deg	±0.15 deg
Total pressure	±75 Pa	±90 Pa
Static pressure	±100 Pa	±130 Pa

The evaluated uncertainty includes systematic and statistical errors of the system. For the present investigation, the systematic errors affect all the measurement results in the same way. Therefore, the uncertainty due to systematic errors has to be subtracted from the values presented in Table 3. They are not relevant in a relative comparison of measurement results, as is presented in this paper.

Casing-Air Injection

The casing-air injection is applied through an injection window that covers a sufficiently representative sector of five rotor pitches. A picture of the injection-window arrangement is shown in Fig. 2. The inner contour of the rotor-casing ring and the injection window were machined together to ensure a continuous inner contour. The part of the window that faces the rotor tip area is interchangeable. In this way, different injection-plate configurations can be tested with a short changeover time.

The cooling air is provided by an air-supply system that dehumidifies the air and controls the temperature and the mass flow. A detailed description of the system can be found in Bernsdorf et al. [36]. To achieve a uniform distribution of the injected air, the injection-window module has a symmetric shape. The air enters the plenum of the module from two sides. To further homogenize the air, the plenum is divided into two chambers. The air enters plenum 1 before it passes through a screen of 3×40 large holes to reach plenum 2. The total pressure and total temperature are measured in plenum 2.

For the present investigation, the axial injection position at 30% rotor axial chord is chosen, because it has given the highest improvement of stage efficiency at the nominal tip gap (Behr et al.

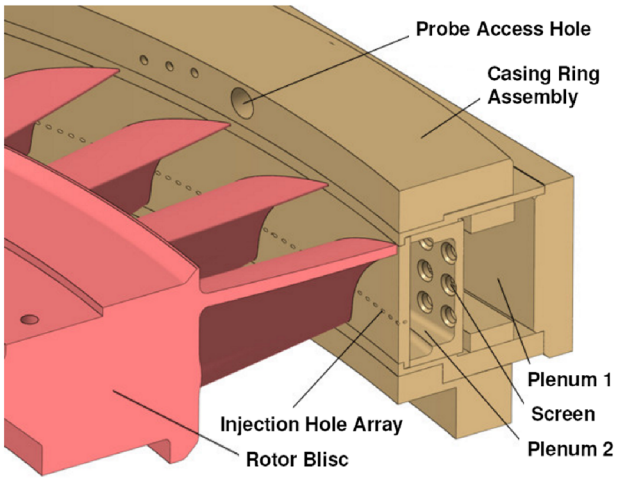

Fig. 2 Air-injection system and probe access within traversable rotor-casing ring assembly.

Table 4 Geometric parameters of injection configurations

Configuration	Small tip gap	Nominal tip gap
Rotor axial chord position at rotor tip, %	30	30
Number of holes/ rotor pitch	10	10
Hole diameter, mm	1.0	1.0
Hole angle relative to casing tangent, deg	30	30
Length/diameter ratio of injection holes	8.0	8.0
Tip gap height, % span	0.65	1.00

Table 5 Injection air conditions

Injection rate, percent of passage mass flow	0.7	1.0
Plenum total pressure $p_{t,I}$, kPa	128	140
Plenum total temperature $T_{t,I}$, °C	32.5	32.5
Average density ratio DR	1.0	1.0
Average blowing ratio BR	2.2	3.2
Average impulse ratio IR	4.8	10.3

[29]). The injection system is designed to counteract the formation of the tip-leakage vortex. Air is injected circumferentially against the rotor turning direction at an angle of 30 deg relative to the casing's tangent to oppose the rotor tip-leakage flow. The selected injection configuration is tested at a nominal tip gap and a small tip gap. The detailed geometry data are listed in Table 4. Both configurations are tested without injection and with injection rates, representing an injection of 0.7% and 1.0% of the turbine mass flow on the full annulus at the conditions shown in Table 5.

Results and Discussion

Baseline Rotor Flowfield

The variation of injection mass flow and tip-gap height will alter the outlet flowfield of the first-stage rotor. To provide an overview of the baseline rotor exit flowfield, the distribution of relative-total-pressure coefficient is presented in Fig. 3. The contour plot shows the sector of two rotor pitches in the rotor-relative frame of reference. This kind of plot is obtained by evaluating the time-resolved probe data measured in the stationary frame of reference and time-averaging them in the rotor-relative frame of reference. The pressure distribution shows regions of low relative total pressure, which are related to the tip-leakage vortex and secondary-flow vortices and the wake of the rotor. The tip-leakage vortex is located at 95% span in close vicinity to the casing endwall. The rotor tip-passage vortex is displaced by the leakage vortex to a span position of around 75% span. In the hub region, the rotor hub-passage vortex is captured by the probe at a span position of around 20%. A pure wake structure appears only at midspan from around 40 to 60% span. A more detailed presentation of the flowfield is given by Behr et al. [30].

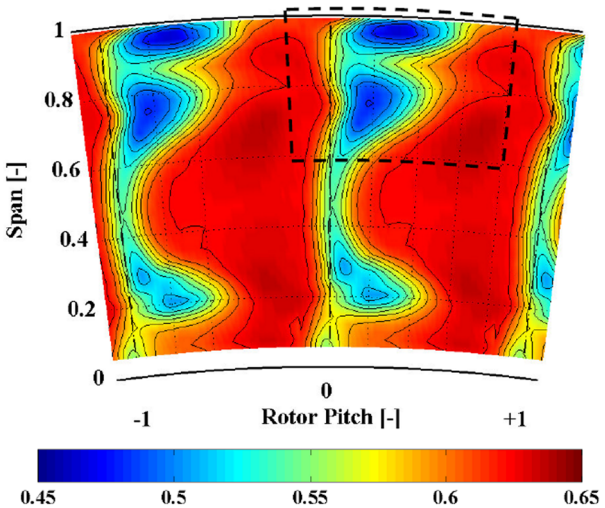

Fig. 3 Relative total pressure coefficient Cp_t measured at 15% axial chord downstream of the rotor at nominal tip gap and no injection (time-averaged in the rotor-relative frame of reference).

This brief discussion makes clear that a region from 60 to 100% span is dominated by vortical structures. A variation of the tip gap and the casing-injection mass flow affects these vortical structures and hence their associated losses and the radial pressure distribution of the rotor exit flow. In the following sections, these effects on flowfield and performance are addressed. The subsequent contour plots of the flowfield will focus on the flow in the tip region and show only the region marked in Fig. 3, which covers the area of one rotor pitch from 60 to 100% span.

Effect of the Tip-Gap Height on the Flowfield

In the present investigation, the tip-gap height is changed from 1.00 to 0.65% of the blade span. This relatively small change causes a change of the rotor exit flow that can be well captured with the applied probe measurement technique. The reduction of the tip clearance allows a smaller fraction of the flow to pass through the blade tip gap. Consequently, the tip-leakage vortex reduces accordingly. This fact is confirmed by the level of turbulence intensity of the tip-leakage vortex, which reduces from the nominal-tip-gap case (Fig. 4a) to the small-tip-gap case (Fig. 5a). In parallel to this, the turbulence intensity of the tip-passage vortex reduces as well. This is due to the fact that both vortices are counter-rotating next to each other. This proximity causes an interaction and dependency of both vortices.

From the contours of turbulence intensity (Figs. 4a and 5a) and from the pitchwise-averaged radial distribution of relative flow angle (Fig. 6a), it is concluded that the vorticity of the tip-leakage vortex has reduced by reducing the tip gap. The line plots in Fig. 6a show the characteristic underturning at around 70% span, caused by the passage vortex, and the flow overturning at around 88% span, caused by both the tip-passage and the tip-leakage vortices. The change of the amplitude of the vortex over- and underturning and the radial shift of the local minimum and maximum confirm the preceding statement concerning the reduction of the vortex strength and diameter with reduced tip clearance.

The aforementioned reduction of turbulence intensity of both vortices with the tip clearance can be seen more clearly in the pitchwise mass-averaged line plots of turbulence intensity of both cases (Fig. 7a). The radial positions of both vortices can be identified by the local maxima at around 75 and 95% span.

In addition, the small tip-clearance case shows a smaller overall mass-averaged relative rotor exit flow angle than the nominal-tip-gap case, which is associated with a higher turning of the rotor by 0.15 deg. Especially from 50 to 70% span, the relative flow angle is smaller by up to 0.5 deg (Fig. 6a).

The effect of the tip-gap height on the flowfield can be summarized as follows. A reduction of the rotor tip gap reduces the strength of the tip-leakage vortex. At the same time, the tip-passage vortex is also attenuated. Consequently, the losses in the rotor are reduced, which is expressed in a higher flow turning across the rotor (Fig. 6a) and lower turbulence (Fig. 7a).

Effect of the Injection Mass Flow on the Flowfield

The effect of the casing-injection mass flow on the rotor flowfield is discussed in detail by Behr et al. [29]. For this reason, only the main effects of the injection are presented in the present paper. The general idea of the concept is to inject casing cooling air from an array of tangentially inclined holes in the rotor casing in a direction opposite to the tip-leakage flow. In this way, the leakage flow and hence the associated losses due to the mixing of the leakage vortex and the main flow are reduced. The fluid that is not injected into the tip gap interacts with the cross-passage flow and influences the development of the passage vortex.

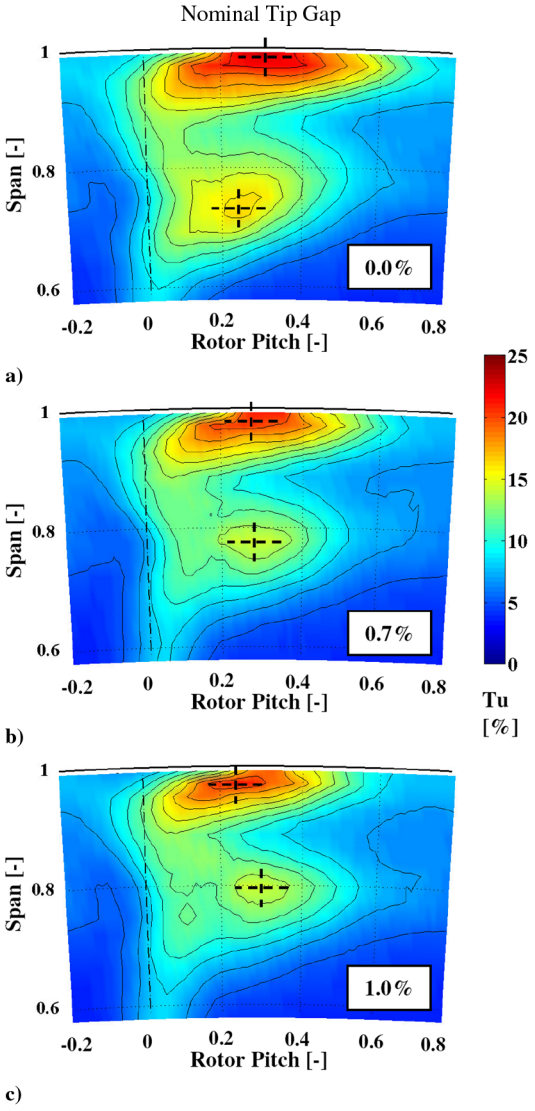

Fig. 4 Turbulence intensity measured at 15% axial chord downstream of the rotor (time-averaged in the rotor-relative frame of reference) with the nominal tip gap at injection rates of a) 0%, b) 0.7%, and c) 1.0%.

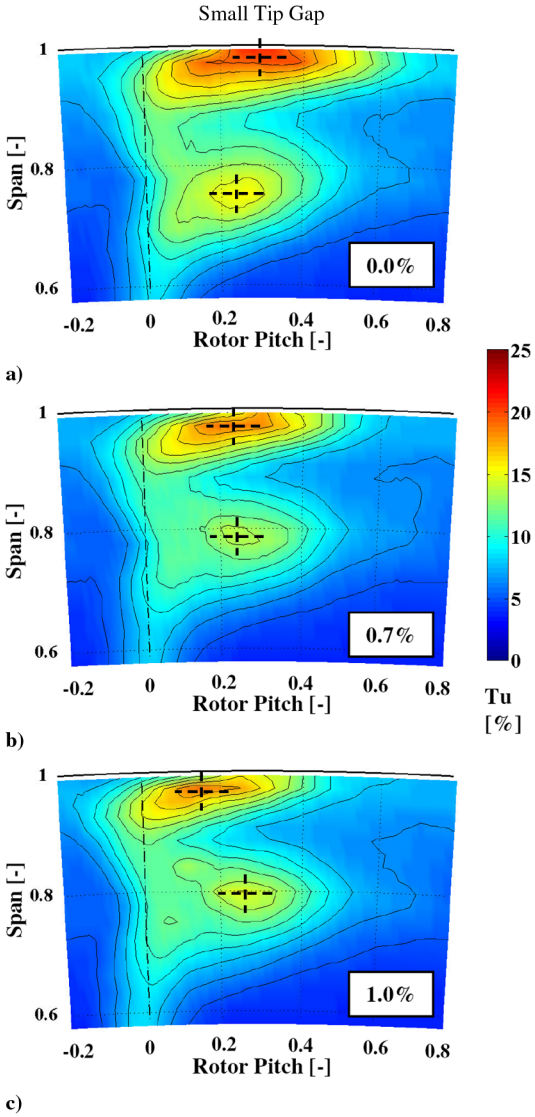

Fig. 5 Turbulence intensity measured at 15% axial chord downstream of the rotor (time-averaged in the rotor-relative frame of reference) with the small tip gap at injection rates of a) 0%, b) 0.7%, and c) 1.0%.

With the casing injection, it was possible to reduce the size of the rotor tip-leakage vortex and the tip-passage vortex. This finding is supported by Fig. 6, which shows the pitchwise-averaged radial distributions of relative flow angle at the rotor exit for the no-injection case and the 0.7 and 1% injection cases. It can be seen in the figure that the radial location of minimum and maximum flow angle moves radially outward with increased injection mass flow. This indicates a reduction of size of the tip-leakage vortex. Consequently, both vortices move toward the tip suction-side corner of the rotor passage. According to this observation, it can be stated that an injection from the casing of 1% of the core mass flow affects the exit flowfield of the rotor from the casing down to around 50% span.

From the radial distribution of relative flow yaw angle at different injection rates, it can be seen that the amplitude of the vortex over- and underturning increases with the injection. It is therefore concluded that the reduction of the vortex size is accompanied by an increase of the vortex rotational speed. It can therefore not be clearly concluded that the vortex strength is also reduced with injection. A possible reason for the increased over- and underturning of the tip-passage vortex with injection can be the reduction of the strength of the tip-leakage vortex, which causes less interaction between the two vortices and, consequently, less diffusion of the tip-passage vortex.

The turbulence intensity of the rotor tip-leakage vortex and the tip-passage vortex reduces with the injection. In the contour plots of turbulence intensity of different injection mass flow cases (Figs. 4 and 5), this trend can clearly be noticed. It was found for the test case with a tip clearance of 1% span that the turbulent kinetic energy (TKE) of the overall rotor exit flowfield reduces linearly with the injection rate. With an injection of 1% of the turbine passage mass flow, the TKE reduces by 25% with respect to the noninjection case.

From the isentropic efficiencies of the injection cases, it can be concluded that the aerodynamic performance of the rotor improves with injection. However, the negative momentum of the injected fluid reduces the work output of the rotor. In [29], the optimum between the two counteracting effects was found at an injection rate of 0.7% of the turbine mass flow at 30% axial chord, which improved the isentropic efficiency by 0.55 percentage points.

Flow Sensitivity on Tip-Gap Height and Injection

After having discussed the separate effects of tip-gap variation and casing-air injection on the rotor flowfield, the combined effect of both will be addressed in this section. From the contour plots of turbulence intensity at different injection rates of the nominal-tip-gap case (Fig. 4) and the small-tip-gap case (Fig. 5), the center positions of the tip-leakage vortex and the tip-passage vortex can be derived by the local maximum of the turbulence level. The relation between the turbulent-loss core of a vortex and its velocity field was investigated by Chaluvadi et al. [37]. The exact positions are marked in the plots

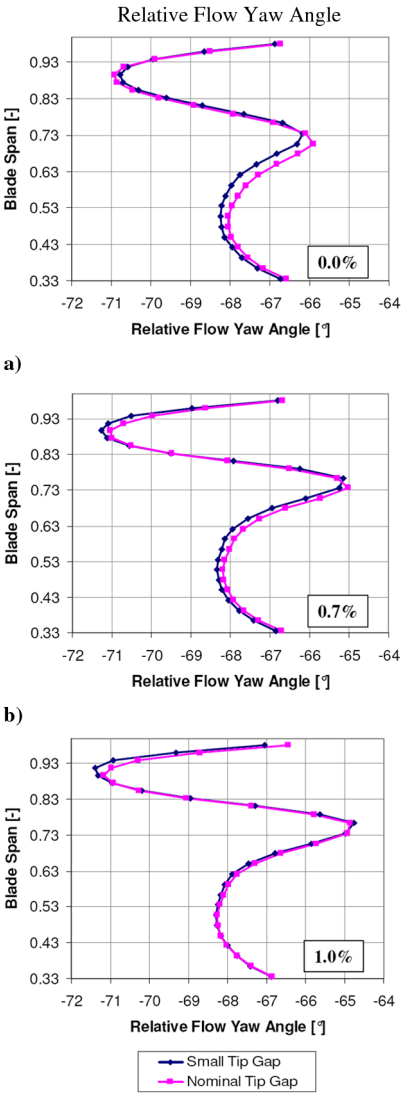

Fig. 6 Spanwise distribution of pitchwise mass-averaged relative flow yaw angle for small and nominal rotor-tip gap at three different injection mass flows in percentage of total turbine mass flow: a) 0%, b) 0.7%, and c) 1%.

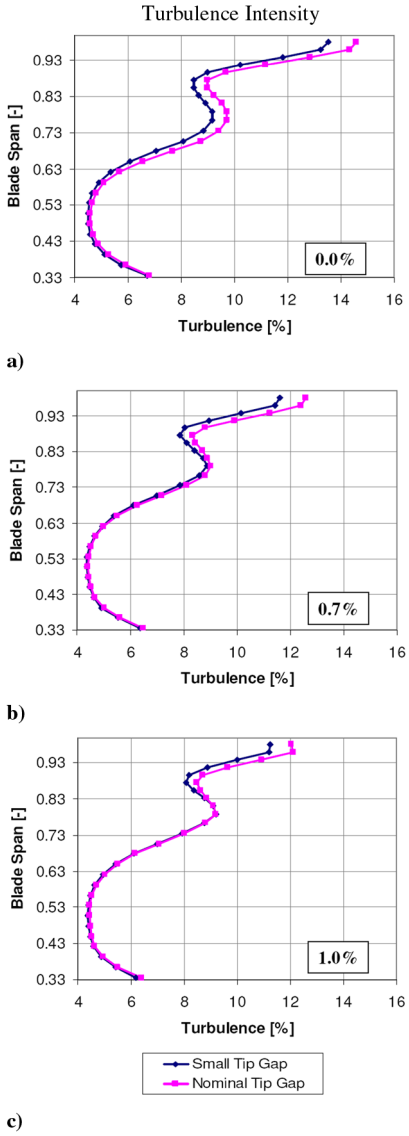

Fig. 7 Spanwise distribution of pitchwise mass-averaged turbulence intensity for small and nominal rotor-tip gap at three different injection mass flows in percentage of total turbine mass flow: a) 0%, b) 0.7%, and c) 1%.

with dashed hairlines. To visualize the dependency of the vortex position on the injection mass flow and the tip-gap size, all vortex positions were transferred in one schematic plot of the same rotor pitch sector (Fig. 8). For the sake of orientation, it shall be said that the wake of the rotor profile is located approximately at the rotor pitch position 0 in the plot. Three positions of each vortex are indicated with symbols, which represent the no-injection case and the injection rates of 0.7 and 1% turbine mass flow. To show the trends, the three symbols of one vortex are connected by a line. The tip-leakage vortex moves with an increasing injection mass flow closer to the trailing of the rotor. The change of the circumferential tip-leakage vortex position between the two cases, no injection and 1% injection, is twice as much for the small-tip-gap case as for the nominal-tip-gap case. With the small tip gap, the vortex position changes by around 15% of a rotor pitch.

The change of the vortex diameters with injection causes a radial displacement of the tip-passage vortex from 73 to 80% span in the nominal-tip-gap case between no injection and 1% injection. A similar effect is observed with the small tip clearance.

Flowfield Desensitization

An interesting side effect of the casing-air injection is observed when applying this technique to cases with different rotor tip clearances. When increasing the injection mass flow up to 1% of the core mass flow, the difference in the radial distributions of relative flow angle and turbulence intensity between both tip-gap cases become smaller. Hence, the injection causes a desensitization of the rotor exit flowfield from the tip-gap height. To visualize the desensitizing effect of the injection on the rotor exit flowfield, the difference in relative exit flow angle of the rotor (Fig. 6) and

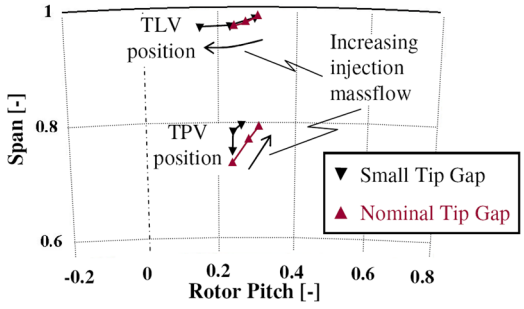

Fig. 8 Change of the center positions of tip-leakage vortex and tip-passage vortex in the rotor-relative frame of reference with injection of 0, 0.7, and 1% of the core mass flow.

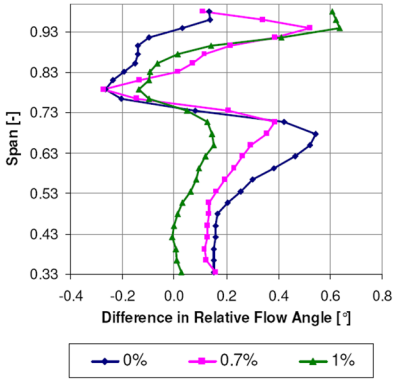

Fig. 9 Difference of relative flow yaw angle between nominal and small tip gap at three injection mass flow rates in percentage of total turbine mass flow.

turbulence intensity (Fig. 7) between both tip-gap cases are presented for different injection rates.

Without injection, the different tip clearance (and hence the different strength and position of the rotor tip vortices) causes an offset in the flow-angle distribution (Fig. 6a), especially from 40 to 80% span. With an injection rate of 1%, this flow-angle difference diminishes (Fig. 6c). A better visualization of the differences in flow angle between the tip-gap cases is given in Fig. 9.

The radial distributions of pitchwise-averaged turbulence intensity show the largest differences between both tip-gap cases without casing injection. This difference occurs from the casing down to 50% span, due to the different characteristics of the rotor tip vortices, which are caused by the difference in the tip-gap height (Fig. 7a). With an injection rate of 1%, the differences in turbulence intensity can be eliminated in the main flowfield until 80% span (Fig. 7c). The reduction of the tip-gap influence on the flowfield turbulence with injection is presented in form of a difference plot in Fig. 10.

Figures 9 and 10 demonstrate that the desensitizing effect of casing-air injection on the flowfield is especially effective in the midspan flow region. In the tip region, which is dominated by the leakage vortex, differences are more difficult to predict.

With the comparison of radial distributions of pitchwise-averaged flow parameters, the desensitizing effect of the injection on the flowfield from the tip-gap height could be shown. The next section will present the effect of the injection on the overall stage performance for the two tip-clearance cases.

Performance Analysis

This section presents performance data of the injection and tip-gap cases investigated. On the basis of these values, the overall effect of the injection on the flowfield and the performance of the turbine can be evaluated.

From the turbulent velocity fluctuations of the flow, the TKE can be derived as

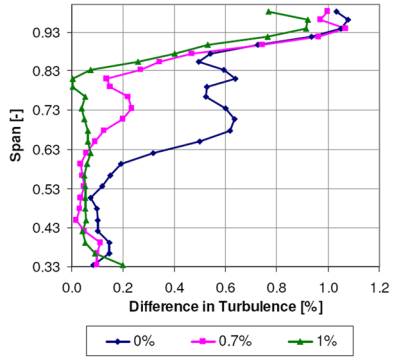

Fig. 10 Difference of turbulence intensity between nominal and small tip gap at three injection mass flow rates in percentage of total turbine mass flow.

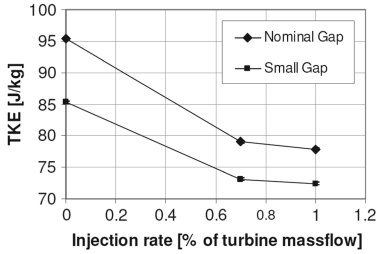

Fig. 11 TKE in joules/kilogram (mass-averaged) versus injection rate percentage of turbine mass flow.

$$\mathrm{TKE} = 0.5 \cdot \left(c'^2_{\mathrm{sw}} + c'^2_r + c'^2_\theta\right)$$

Figure 11 shows the relation between the TKE and the injection rate. The plot shows mass-averaged values to account for the mass flow redistribution in the flowfield due to the injection. Generally, it can be stated that the mass-averaged value of TKE reduces with injection. The nominal- and the small-tip-gap cases show a reduction of 18 and 15%, respectively, at an injection rate of 1%, compared with the no-injection case. The difference in TKE between both tip-gap cases halves with an injection rate of 1%, compared with the no-injection case, which therefore verifies the desensitizing character of the casing injection.

In the following, the efficiencies of the injection cases are analyzed to evaluate the overall effect of the casing injection on the performance of the turbine at different tip-gap heights. The aerodynamic efficiency can be defined as the ratio of the real and isentropic enthalpy flux difference:

$$\eta = \frac{\Delta \dot{H}_{\mathrm{real}}}{\Delta \dot{H}_{\mathrm{is}}}$$

where

$$\Delta \dot{H} = \dot{m}(h_{t,\mathrm{in}} - h_{t,\mathrm{out}}), \qquad h_t = c_p T_t$$

If various mass flows of different total temperature and pressure are involved in the expansion process, as in case of cooling injection, a general definition can be formulated:

$$\eta = \frac{\sum_{i=1}^{I} \dot{m}_i c_p T_{t,i} - \sum_{j=1}^{J} \dot{m}_j c_p T_{t,j}}{\sum_{i=1}^{I} \dot{m}_i c_p T_{t,i} - \sum_{j=1}^{J} \dot{m}_j c_p T_{t,\mathrm{is},j}}$$

with

$$T_{t,\mathrm{out,is}} = T_{t,\mathrm{in}} \left(\frac{p_{t,\mathrm{out}}}{p_{t,\mathrm{in}}}\right)^{\frac{\kappa-1}{\kappa}}$$

For each mass flow fraction the isentropic exit temperature can be derived based on the total pressure ratio and the inlet total temperature.

In the current cases, the turbine inlet mass flow $\dot{m}_M$ and the injection mass flow $\dot{m}_I$ are introducing energy into the system. The sum of both mass flows $\dot{m}_T = \dot{m}_M + \dot{m}_I$ leaves the rotor. The total temperatures and total pressures of the passage mass flows were measured with FRAP. The 2-D temperature and pressure data of each plane are mass-averaged values. The values of the injection mass flow were measured inside the plenum with three PT100 sensors and three total pressure sensors.

According to the preceding equations, a thermodynamic isentropic efficiency value can be defined for the current case as follows:

$$\eta = \frac{\dot{m}_M c_p \bar{T}_{t,M} + \dot{m}_i c_p \bar{T}_{t,I} - \dot{m}_T c_p \bar{T}_{t,T}}{\dot{m}_M c_p \bar{T}_{t,M}\left(1 - \left((\bar{p}_{t,T})/(\bar{p}_{t,M})\right)^{\frac{\kappa-1}{\kappa}}\right) + \dot{m}_I c_p \bar{T}_{t,I}\left(1 - \left((\bar{p}_{t,T})/(\bar{p}_{t,I})\right)^{\frac{\kappa-1}{\kappa}}\right)}$$

The change of efficiency with injection for both tip-gap cases is presented in Fig. 12. The standard uncertainty of the efficiency

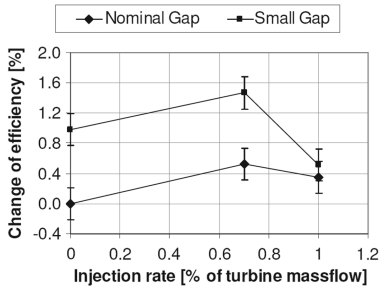

Fig. 12 Isentropic efficiency percentage of nominal and small-tip-gap case as the difference from the nominal-tip-gap case without injection versus injection rate percentage of turbine mass flow.

values with a coverage of 66% is stated by the error bars in the plot. The flow mechanisms that are responsible for the maximum in efficiency at the 0.7% injection case are explained in detail by Behr et al. [29].

Without injection, the efficiency of the small-tip-gap case is around one percentage point higher than that of the nominal-tip-gap case. That means that a change of tip clearance of 0.35% span causes a change of efficiency of around 1%. This ratio is confirmed by another investigation of Behr [34] in the same turbine configuration. In this study, two tip gaps are investigated by changing the diameter of the rotor. The mechanic efficiency is obtained by using the torque measured on the turbine shaft.

With an injection rate of 0.7%, the efficiency of both tip-gap cases increases by around 0.5 percentage points. At an injection rate of 1% of the turbine mass flow, the efficiency values of both tip-gap cases collapse to almost the same value. At this injection rate, the tip-gap influence on the stage efficiency is eliminated.

Conclusions

This study presents an experimental investigation of using rotor-casing cooling air to desensitize the flowfield of the rotor and the performance of the stage from the tip-gap height. The cooling air is injected through discrete holes from the rotor casing in a circumferential direction at a 30-deg angle from the casing tangent. The injection is oriented to oppose the tip-leakage flow of the rotor. Two rotor tip-gap heights of 0.65 and 1% span are investigated at injection rates of up to 1% of the turbine mass flow. Fast-response pressure probes are used to measure the rotor exit flowfield.

It is shown that the injected air influences the development of the rotor tip-leakage vortex and the rotor tip-passage vortex in such a way that the main flowfield shows no measurable effect from the change of tip gap. Without injection, the radial distribution of relative rotor exit angles differs between both tip-gap cases by up to 0.5 deg. With the injection of a cooling-air mass flow of 1% of the turbine mass flow, these differences are reduced to below 0.1 deg in the main flowfield until 80% span.

The turbulence intensity of the rotor tip vortices reduces linearly with the injection mass flow. The difference between both tip-gap cases in overall turbulent kinetic energy of the rotor exit flowfield halves with an injection rate of 1%, compared with the no-injection case.

The differences in the flowfield between different tip-gap cases are caused by the different tip-leakage and secondary-flow structures associated with the tip-gap size. With the injection of casing air, the tip-leakage vortex and the tip-passage vortex are altered in such a way that they influence the main flow in a similar manner.

The evaluation of stage efficiency shows an equalization of the efficiency values of both tip-gap cases at an injection rate of 1%. At this injection rate, the efficiency of the larger tip-gap case is increased by 0.35 percentage points, compared with the no-injection case.

The method of cooling-air injection from the rotor casing is suggested as a tool to achieve a constant flowfield at different tip-gap heights, which allows a better optimization of the turbine flow path geometry.

References

[1] Booth, T. C., Dodge, P. R., and Hepworth, H. K., "Rotor-Tip Leakage Part 1: Basic Methodology," *Journal of Engineering for Power*, Vol. 104, 1982, pp. 154–161.

[2] Wiseman, M. W., and Guo, T., "An Investigation of Life Extending Control Techniques for Gas Turbine Engines," *Proceedings of the American Control Conference*, Vol. 5, IEEE Service Center, Piscataway, NJ, 2001, pp. 3706–3707.

[3] Lattime, S. B., and Steinetz, B. M., "High-Pressure-Turbine Clearance Control Systems: Current Practices and Future Directions," *Journal of Propulsion and Power*, Vol. 20, No. 2, 2004, pp. 302–311. doi:10.2514/1.9255

[4] Harvey, N. W., "Aerothermal Implications of Shroudless and Shrouded Blades," *Turbine Blade Tip Design and Tip Clearance Treatment*, VKI Lectures Series 2004-02, Vol. 1, von Karman Inst. for Fluid Dynamics, Rhode-Saint-Genèse, Belgium, 2004.

[5] Denton, J. D., "The 1993 IGTI Scholar Lecture: Loss Mechanisms in Turbomachines," *Journal of Turbomachinery*, Vol. 115, No. 4, 1993, pp. 621–656. doi:10.1115/1.2929299

[6] Booth, T. C., "Importance of Tip Leakage Flows in Turbine Design," *Tip Clearance Effects in Axial Turbomachines*, VKI Lecture Series 1985-05, von Karman Inst. for Fluid Dynamics, Rhode-Saint-Genèse, Belgium, 1985.

[7] Bindon, J. P., and Morphis, G., "The Development of Axial Turbine Leakage Loss for Two Profiled Tip Geometries Using Linear Cascade Data," American Society of Mechanical Engineers Paper 90-GT-152, June 1990.

[8] Kaiser, I., and Bindon, J. P., "The Effect of Tip Clearance on the Development of Loss Behind a Rotor and a Subsequent Nozzle," American Society of Mechanical Engineers Paper 97-GT-53, 1997.

[9] Camci, C., Dey, D., and Kavurmacioglu, L., "Tip Leakage Flows in Near Partial Squealer Rims in an Axial Flow Turbine Stage," American Society of Mechanical Engineers Paper GT2003-38979, 2003.

[10] Mischo, B., Behr, T., and Abhari, R. S., "Flow Physics and Profiling of Recessed Balde Tips: Impact on Performance and Heat Load," American Society of Mechanical Engineers Paper GT2006-91074, 2006.

[11] Tallman, J. A., "A Computational Study of Tip Desensitization in Axial Flow Turbines, Part 2: Turbine Rotor Simulations With Modified Tip Shapes," American Society of Mechanical Engineers Paper GT2004-53919, 2004.

[12] Willer, L., Haselbach, F., and Newman, D. A., "An Investigation Into a Novel Turbine Rotor Winglet: Part 2—Numerical Simulation and Experimental Results," American Society of Mechanical Engineers Paper GT2006-90459, 2004.

[13] Schabowski, Z., and Hodson, H., "The Reduction of Over Tip Leakage Loss in Unshrouded Axial Turbines Using Winglets and Squealers," American Society of Mechanical Engineers Paper GT2007-27623, 2007.

[14] Chander, P., Lee, C.-P., Cherry, D., Wadia, A., and Doughty, R., "Analysis of Some Improved Blade Tip Concepts," American Society of Mechanical Engineers Paper GT2005-68333, 2005.

[15] De Cecco, S., Yaras, M. I., and Sjolander, S. A., "Measurement of Tip Leakage Flows in Turbine Cascade with Large Clearances," American Society of Mechanical Engineers Paper 95-GT-77, June 1995.

[16] Yamamoto, A., Tominaga, J., Matsunuma, T., and Outa, E., "Detailed Measurements of Three-Dimensional Flows and Losses Inside an Axial Flow Turbine Rotor," American Society of Mechanical Engineers Paper 94-GT-348, June 1994.

[17] Staubach, J. B., Sharma, O. P., and Stetson, G. M., "Reduction of Tip Clearance Losses Through 3-D Airfoil Designs," American Society of Mechanical Engineers Paper 96-TA-13, November 1996.

[18] Offenburg, L. S., Fischer, J. D., and Hoek, T. J. V., "An Experimental Investigation of Turbine Case Treatments," AIAA Paper 87-1919, June 1987.

[19] Kolthoff, P., "Device for Controlling Clearance Between Rotor and Shroud of a Turbine," U.S. Patent 3,039,737, 1962.

[20] Schwarz, F. M., "Seal Clearance Control System for a Gas Turbine," U.S. Patent 4,213,296, 1980.

[21] Tseng, W., and Hauser, A. A., "Blade Tip Clearance Control Apparatus with Shroud Segment Position Adjustment by Unison Ring Movement," U.S. Patent 5,035,573, 1981.

[22] Catlow, R., "Blade Tip Clearance Control Apparatus," U.S. Patent 5,211,534, 1993.

[23] Carpenter, K. D., Wiedemer, J. D., and Smith, P. A., "Rotor Blade Outer Tip Seal Apparatus," U.S. Patent 5,639,210, 1997.

[24] Huber, F. W., and Dietrich, D. J., "Clearance Control for the Turbine of

a Gas Turbine Engine," U.S. Patent 5,667,359, 1997.
[25] Dey, D., and Camci, C., "Development of Tip Clearance Flow Downstream of a Rotor Blade with Coolant Injection from a Tip Trench," *8th International Symposium on Transport, Phenomena and Dynamic of Rotating Machinery (ISROMAC-8)*, 2000, pp. 572–579.
[26] Rao, N. M., and Camci, C., "Axial Turbine Tip Desensitization by Injection from a Tip Trench, Part 1: Effect of Injection Mass Flow Rate," American Society of Mechanical Engineers Paper GT2004-53256, 2004.
[27] Auyer, E. L., "Dynamic Sealing Arrangement for Turbomachines," U.S. Patent No. 2,685,429, 1954.
[28] Minoda, M., Inoue, S., Usui, H., and Hiroyuki, N., "Air Sealed Turbine Blades," U.S. Patent No. 4,732,531, 1988.
[29] Behr, T., Kalfas, A. I., and Abhari, R. S., "Control of Rotor Tip Leakage through Cooling Air Injection from the Casing in a High-Work Turbine: Experimental Investigation," *Journal of Turbomachinery*, American Society of Mechanical Engineers Paper GT2007-27269, Vol. 129, 2007.
[30] Behr, T., Kalfas, A. I., and Abhari, R. S., "Unsteady Flow Physics and Performance of a One-and-1/2-Stage Unshrouded High Work Turbine," *Journal of Turbomachinery*, Vol. 129, No. 2, 2007, pp. 348–359.
doi:10.1115/1.2447707
[31] Kupferschmied, P., Köppel, O., Gizzi, W. P., and Gyarmathy, G., "Time Resolved Flow Measurements with Fast Aerodynamic Probes in Turbomachinery," *Measurement Science and Technology*, Vol. 11, No. 7, 2000, pp. 1036–1054.
doi:10.1088/0957-0233/11/7/318
[32] Pfau, A., Schlienger, J., Kalfas, A. I., and Abhari, R. S., "Unsteady, 3-Dimensional Flow Measurement Using a Miniature Virtual 4 Sensor Fast Response Aerodynamic Probe (FRAP)," American Society of Mechanical Engineers, Paper GT2003-38128, 2003.
[33] Porreca, L., Hollenstein, M., Kalfas, A. I., and Abhari, R. S., "Turbulence Measurements and Analysis in a Multistage Axial Turbine," *Journal of Propulsion and Power*, Vol. 23, No. 1, 2007, pp. 227–234.
doi:10.2514/1.20022
[34] Behr, T., "Control of Rotor Tip Leakage and Secondary Flow by Casing Air Injection in Unshrouded Axial Turbines," Ph.D. Thesis No. 17283, ETH Zurich, Zurich, 2007.
[35] *Guide to the Expression of Uncertainty in Measurement*, 1st ed., International Organization for Standardization, Geneva, 1993.
[36] Bernsdorf, S., Rose, M. G., and Abhari, R. S., "Modeling of Film Cooling, Part 1: Experimental Study of Flow Structure," *Journal of Turbomachinery*, Vol. 128, No. 1, 2006, pp. 141–149.
doi:10.1115/1.2098768
[37] Chaluvadi, V. S. P., Kalfas, A. I., Banieghbal, M. R., Hodson, H. P., and Denton, J. D., "Blade Row Interaction in a High-Pressure Turbine," *Journal of Propulsion and Power*, Vol. 174, July–Aug. 2001, pp. 892–901.

A. Prasad
Associate Editor